



Article

Pipicolisporin, a Novel Cyclic Peptide with Antimalarial and Antitrypanosome Activities from a Wheat Endophytic *Nigrospora oryzae*

Ignacio Fernández-Pastor ¹, Víctor González-Menéndez ¹, Frederick Annang ¹, Clara Toro ¹, Thomas A. Mackenzie ¹, Cristina Bosch-Navarrete ², Olga Genilloud ¹ and Fernando Reyes ^{1,*}

- ¹ Fundación MEDINA, Centro de Excelencia en Investigación de Medicamentos Innovadores de Andalucía, Parque Tecnológico de Ciencias de la Salud, Avda. del Conocimiento 34, 18016 Granada, Spain; ignacio.fernandez@medinaandalucia.es (I.F.-P.); victor.gonzalez@medinaandalucia.es (V.G.-M.); freddie.annang@medinaandalucia.es (F.A.); clara.toro@medinaandalucia.es (C.T.); thomas.mackenzie@medinaandalucia.es (T.A.M.); olga.genilloud@medinaandalucia.es (O.G.)
- ² Instituto de Parasitología y Biomedicina “López-Neyra”, Consejo Superior de Investigaciones Científicas (CSIC) Avda. del Conocimiento 17, Armilla, 18016 Granada, Spain; cristinabosch@ipb.csic.es
- * Correspondence: fernando.reyes@medinaandalucia.es; Tel.: +34-958-993965

Abstract: A novel cyclic antimalarial and antitrypanosome hexapeptide, pipicolisporin (**1**), was isolated from cultures of *Nigrospora oryzae* CF-298113, a fungal endophyte isolated from roots of *Triticum* sp. collected in a traditional agricultural land of Montefrío, Granada, Spain. The structure of this compound, including its absolute configuration, was elucidated by HRMS, 1-D and 2-D NMR spectroscopy, and Marfey’s analysis. This metabolite displayed interesting activity against *Plasmodium falciparum* and *Trypanosoma cruzi*, with IC₅₀ values in the micromolar range, and no significant cytotoxicity against the human cancer cell lines A549, A2058, MCF7, MIA PaCa-2, and HepG2.

Keywords: pipicolisporin; *Nigrospora oryzae*; fungal endophyte; structural elucidation; Marfey’s analysis; antiparasitic activity



Citation: Fernández-Pastor, I.; González-Menéndez, V.; Annang, F.; Toro, C.; Mackenzie, T.A.; Bosch-Navarrete, C.; Genilloud, O.; Reyes, F. Pipicolisporin, a Novel Cyclic Peptide with Antimalarial and Antitrypanosome Activities from a Wheat Endophytic *Nigrospora oryzae*. *Pharmaceuticals* **2021**, *14*, 268. <https://doi.org/10.3390/ph14030268>

Academic Editor: Marcelo J. Nieto

Received: 22 February 2021

Accepted: 13 March 2021

Published: 16 March 2021

Publisher’s Note: MDPI stays neutral with regard to jurisdictional claims in published maps and institutional affiliations.



Copyright: © 2021 by the authors. Licensee MDPI, Basel, Switzerland. This article is an open access article distributed under the terms and conditions of the Creative Commons Attribution (CC BY) license (<https://creativecommons.org/licenses/by/4.0/>).

1. Introduction

Mutualism between plants and fungal endophytes is almost universal; indeed, no study has yet reported the existence of any plant species without endophytes [1,2]. Endophytes can be a double-edged sword, as they usually act to protect the host against other phytopathogens, but they may act as opportunistic pathogens during plant senescence or under stress conditions [3–5]. Although an enormous diversity of endophyte metabolites and their biological activities have so far been reported, only about 10% of the approximately one million known terrestrial endophytes have been investigated [6].

According to the WHO report in 2020, vector-borne diseases account for more than 17% of all infectious diseases, causing more than 700,000 deaths annually. Protozoan parasites, such as *Plasmodium falciparum* or *Trypanosoma cruzi*, are the cause of malaria and Chagas disease, respectively, and it is estimated that approximately a billion people around the world suffer from these diseases every year [7].

Although historically plants have been the main source of antiplasmodial natural products [8], many antimicrobial secondary metabolites from fungal endophytes have also been described as potential antiprotozoal agents. These include, among others, altenusin [9], xylariaquinone A [10], codinaeopsin [11], fusaripeptide A [12], strasseriolides A–D [13], leucinostatins [14], griseofulvin [15], or trichodermin [16]. Other interesting biological properties exhibited by endophytic metabolites include antifungal, anti-inflammatory, antiproliferative, or anticancer activities [17].

The increasing resistance of parasites to conventional drugs makes the research of new and more specific bioactive molecules mandatory, and the discoveries of venturamide

A [18], cyclosporin A derivatives [19], and kakeromamide B [20] are examples of this. Cyclic peptides possess several favorable pharmacological features as antiparasitic natural products [21] and their solid-phase synthesis offers a unique advantage for further optimization of the initial hits guided by medicinal chemistry [22].

As a result of the LC/MS survey of new fungal metabolites in extracts from cultures of crop endophytes, we identified an intense peak with the not previously reported molecular formula $C_{37}H_{53}N_7O_6$ in a culture in solid rice-based medium (BRFT) of the strain CF-298113 of *Nigrospora oryzae*, isolated from roots of *Triticum* sp. collected in a traditional cropland in Spain. The fungus *N. oryzae* is a common endophyte in plants and algae, and only a few natural products have been previously reported from this species. The most remarkable ones are the antibacterial nigrosporins A and B [23], quercetin monoglycosides [5], and the cyclohexadepsipeptides oryzamides A–E [24]. The novelty of the new molecule identified in our *N. oryzae* strain together with the scarce number of compounds isolated from this fungal species prompted us to investigate its chemical structure and biological properties.

2. Results and Discussion

2.1. Isolation and Structural Elucidation of Pipecolisporin

Fractionation of the methyl ethyl ketone (MEK) extract of a scaled-up culture of *N. oryzae* CF-298113 in BRFT medium (Figure S1), using reversed-phase C18 medium pressure chromatography followed by semipreparative reversed-phase HPLC on a phenyl column, resulted in the isolation of pipecolisporin (**1**) (Figure 1).

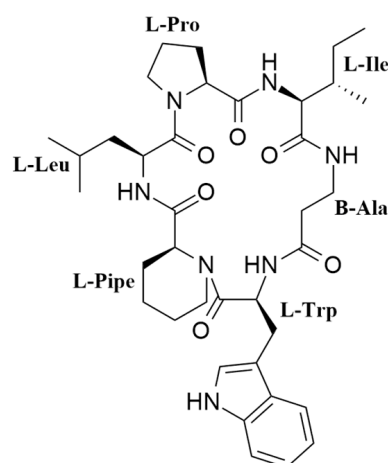


Figure 1. Structure of pipecolisporin (**1**).

Compound **1** was obtained as a white amorphous solid. A molecular formula $C_{37}H_{53}N_7O_6$ was deduced from its (+)-ESI-TOF analysis ($[M + H]^+$ 692.4152, Δ +3.2 ppm) (Figure S3). NMR spectroscopy was extensively applied to determine the structure of the peptide. The 1H spectrum of **1** (Figure S5) exhibited characteristic signals for multiple exchangeable protons (δ_H 7.0–11.0 ppm), six signals of α -hydrogens of amino acids (δ_H 3.8–4.6 ppm), and different alkyl (δ_H 0.6–3.8 ppm) or aromatic (δ_H 6.9–7.6 ppm) side chain hydrogens. Analysis of COSY and TOCSY spectra (Figures S9 and S10, respectively) allowed the identification of spin systems consistent with the presence of the following proteinogenic amino acids: Trp ($\times 1$), Ile ($\times 1$), Leu ($\times 1$), and Pro ($\times 1$). It also accounted for the presence of one β -Alanine residue (β -Ala) and one pipecolic acid residue (Pipe). The cyclic nature of the peptide and the connectivity between amino acids was confirmed by the key NOESY and HMBC correlations shown in Figure 2, additionally supported by HRMS/MS fragmentation experiments (Figure 3).

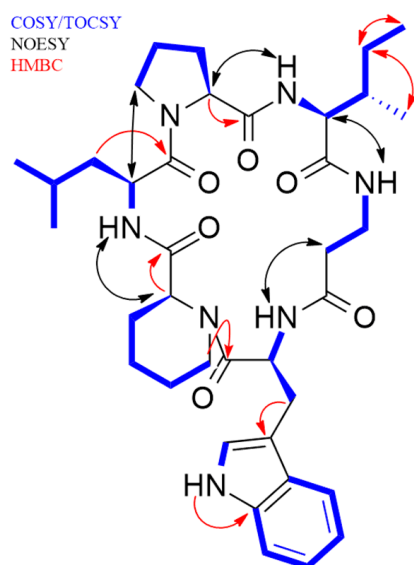
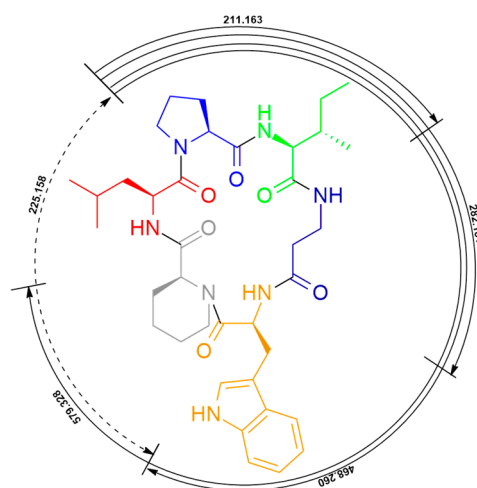
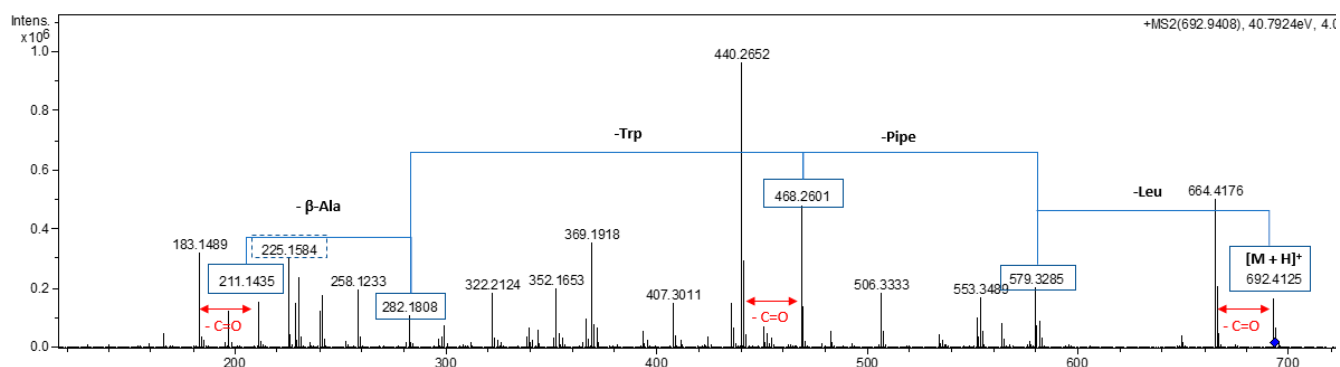


Figure 2. Key ^1H - ^1H COSY, TOCSY, NOESY, and HMBC correlations for pipecolisporin (1).



(a)



(b)

Figure 3. ESI-TOF MS/MS fragmentation of pipecolisporin (1). (a) Relevant fragments found. (b) MS/MS spectrum with the most relevant fragments highlighted.

Marfey's analysis allowed the determination of the absolute configuration of all the amino acid residues as L. For this aim, the retention time of L and D standards of all the amino acids present in the peptide derivatized with L-FDVA, namely Pro, Ile, Leu, Trp, and Pip, were compared with the retention time of a hydrolyzed and derivatized aliquot of **1** (Figures S12 and S13). Additionally, due to the coelution of L-Ile and L-*allo*-Ile in the analytical LC/MS conditions employed, the presence of L-Ile in the structure was confirmed by comparison of the HSQC NMR spectra of a hydrolysate of **1** with those of L-Ile and L-*allo*-Ile standards (Figures S14 and S15), a strategy recently employed in the determination of the absolute configuration of Ile residues in cacaoidin [25].

2.2. Biological Activity

The isolated compound was tested against several tropical parasites and exhibited activity in the micromolar range against *P. falciparum* 3D7 and *T. cruzi* Tulahuen C4 parasites. The activity versus the *T. cruzi* Tulahuen C4 parasites was the most remarkable, with a measured IC₅₀ of 8.46 μM, comparable to that of the standard drug benznidazole, currently used in the treatment of Chagas disease (IC₅₀ in the same assay of 2.21 μM) (Figures S16 and S17). The activity measured against *P. falciparum* was also in the micromolar range, with an IC₅₀ of 3.21 μM (Figure S18). When tested against the human cancer cell lines A549 (lung carcinoma), A2058 (metastatic melanoma), MCF7 (breast adenocarcinoma), MIA PaCa-2 (pancreatic carcinoma), and HepG2 (hepatocyte carcinoma) by means of a cell viability MTT assay, the compound was found to not be cytotoxic at the highest concentration tested of 50 μM (Figure S20). Additionally, the compound was tested against a panel of microbial human pathogens, including Gram positive (methicillin-resistant *Staphylococcus aureus*, MRSA), Gram negative (*Acinetobacter baumannii*, *Eschericia coli*, and *Pseudomonas aeruginosa*), yeast (*Candida albicans*), and fungi (*Aspergillus fumigatus*), and proved to not be active against any of them at a concentration of 128 μg/mL.

3. Materials and Methods

3.1. General Experimental Procedures

Solvents employed were all HPLC grade. Optical rotations were measured on a Jasco P-2000 polarimeter (JASCO Corp., Tokyo, Japan). IR spectra were recorded with a JASCO FT/IR-4100 spectrometer (JASCO Corp.) equipped with a PIKE MIRacle™ single reflection ATR accessory. LC-UV-LRMS analyses were performed on an Agilent 1260 Infinity II (Agilent Technologies, Santa Clara, CA, USA) single quadrupole LC-MS system. HRESIMS and MS/MS spectra were acquired using a Bruker maXis QTOF mass spectrometer (Bruker Daltonik GmbH, Bremen, Germany) coupled to an Agilent 1200 Rapid Resolution HPLC. The mass spectrometer was operated in positive and negative mode. Medium pressure liquid chromatography (MPLC) was performed on a CombiFlash Teledyne ISCO Rf400x apparatus (Teledyne ISCO, Lincoln, NE, USA) with a preloaded C18 column (Phenomenex, 50 μm). Preparative or semi-preparative HPLC purifications were performed on a Gilson GX-281 322H2 HPLC (Gilson Technologies, Middleton, WI, USA) using reversed-phase semi-preparative (XBridge, Phenyl, 10 × 150 mm, 5 μm) column. 1-D and 2-D NMR spectra were recorded at 297 K on a Bruker Avance III spectrometer (500 and 125 MHz for ¹H and ¹³C, respectively) equipped with a 1.7-mm TCI MicroCryoProbe™ (Bruker Biospin, Fällanden, Switzerland). ¹H and ¹³C chemical shifts were reported in ppm using the signals of the residual solvents as internal reference (δ_H 2.50 and δ_C 39.52 ppm for DMSO-*d*₆; δ_H 4.75 ppm for D₂O).

3.2. Microbial Isolation and Identification

The producer strain CF-298113 was isolated from surface disinfected root pieces of *Triticum* sp. collected in a traditional agricultural land in Montefrío (Granada, Spain) following a previously described standard indirect technique [26]. The axenic strain was preserved as frozen suspensions of septate mycelium and conidia in 10% glycerol at $-80\text{ }^{\circ}\text{C}$. This strain is currently maintained in the Fungal Culture Collection of Fundación MEDINA (<http://www.medinadiscovery.com>). DNA extraction, PCR amplification, and DNA sequencing were performed as previously described [26]. Sequences of the complete ITS1-5.8S-ITS2 and initial 28S region or independent ITS and partial 28S rDNA were compared with those deposited at GenBank or the NITE Biological Resource Center (<http://www.nbrc.nite.go.jp/>) by using the BLAST application [27,28]. Database matching with the ITS rDNA sequence (www.fungalbarcode.org) yielded a complete sequence similarity (100%) to the strain of *Nigrospora oryzae* ATCC 12,772 GenBank Accession No. KU933443), thus indicating that strain CF-298113 was genetically similar to *N. oryzae*, and conspecific. High similar scores to other authentic fungal strains of this species, e.g., *N. oryzae* CBS 113884 [29] (GenBank Accession No. DQ219433, 100% sequence similarity), or *N. oryzae* CBS 231.32 (GenBank Accession No. MH855300, 99% sequence similarity) indicated that CF-298113 can be classified as *Nigrospora oryzae* (Berk. & Broome).

3.3. Fungal Solid-State Fermentation (SSF)

Strain CF-298113 was fermented by inoculating 10 mycelial agar plugs into SMYA medium (Bacto neopeptone 10 g; maltose 40 g; yeast extract 10 g; agar 3 g; H_2O 1 L) in two flasks (50 mL of medium in a 250-mL Erlenmeyer). The flasks were incubated on a rotary shaker at 220 rpm at $22\text{ }^{\circ}\text{C}$ with 70% relative humidity. After growing the seed stage for 7 days, aliquots of 4 mL were used to inoculate $20 \times 500\text{-mL}$ Erlenmeyer flasks containing the production solid rice-based medium (BRFT). The BRFT medium contained 20 g of brown rice and 40 mL of a solution of yeast extract 1 g/L, sodium tartrate 0.5 g/L and KH_2PO_4 0.5 g/L per flask [30]. The 20 flasks seeded were incubated under static conditions at $22\text{ }^{\circ}\text{C}$ and 70% relative humidity for 21 days. The resulting 20 solid flask fermentations were extracted by adding MEK ($20 \times 100\text{ mL}$) and 20 mL of HPLC quality water to each flask. Then, the flasks were shaken in a Kühner at 220 rpm for 1 h. After that, the mixtures were centrifuged (10 min, 9000 rpm) and filtered under vacuum. All solutions were pooled into a separation funnel and the organic extract was rotary evaporated until dry (40 g).

3.4. Isolation and Identification of Pipecolisporin

The solid residue obtained was mixed with reversed phase C-18 silica gel in a 1:2 ratio and loaded onto a C-18 column ($200 \times 35\text{ mm}$) that was eluted with a stepped $\text{H}_2\text{O-CH}_3\text{CN}$ gradient (18 mL/min; 0–100% CH_3CN in 55 min; UV detection at 210 nm and 280 nm). Those fractions containing **1**, as confirmed by LC/MS analysis, were re-purified by semi-preparative RP-HPLC (X-Bridge, Phenyl, $10 \times 150\text{ mm}$, 5 μm) applying isocratic elution of $\text{H}_2\text{O-CH}_3\text{CN}$ as mobile phase (3.6 mL/min; 32% CH_3CN for 40 min; UV detection at 210 nm). Fractions containing the peak eluting at 18–20 min were pooled, the organic solvent was evaporated under a N_2 stream, and the resulting aqueous solution was freeze-dried. Pipecolisporin (**1**) was thus obtained as an amorphous white powder (10 mg).

Pipecolisporin (**1**): white amorphous solid; $[\alpha]_{\text{D}} -33.0$ (c 0.013, MeOH); UV (DAD) 210, 290 nm; IR (ATR) ν_{max} 3344, 2936, 2871, 1644, 1539, 1443, 1263, 1024 and 743 cm^{-1} , ^1H and ^{13}C NMR data see Table 1, (+)-ESI-TOF m/z 692.4152 $[\text{M} + \text{H}]^+$ (calcd for 692.4130), 709.4417 $[\text{M} + \text{NH}_4]^+$ (calcd for 709.4396) and 1400.8444 $[2\text{M} + \text{NH}_4]^+$ (calcd for 1400.8453).

Table 1. NMR data of pipecolisporin (**1**) in DMSO-*d*₆.

Amino Acid	Position	δ H, m, J (Hz)	δ C, Mult	HMBC (H to C)	NOESY
Pro	1	3.99, m	62.9, CH	CO Pro	NH Ile
	2	2.19, m, 1.77, m	29.4, CH ₂	CO Pro	
	3	1.99, m, 1.84, m	25.7, CH ₂		
	4	3.72, m 3.56, m	47.3, CH ₂		Leu 1
	CO		171.8, C		
Ile	NH amide	6.47, d, (8.0)		Pro 1	
	1	4.01, m	57.5, CH		NH β -Ala
	2	1.91, m	37.0, CH		
	3	1.30, m, 1.08, m	24.7, CH ₂		
	4	0.82, m	12.1, CH ₃	Ile 3	
	2-Me	0.81, m	16.2, CH ₃	Ile 3	
β -Ala	CO		171.2, C		
	NH amide	7.05, m		CO Ile	Ile 1
	1	2.43 m, 2.11, m	35.2 CH ₂		
	2	3.71, m, 3.12, m	35.0, CH ₂		NH Trp
Trp	CO		171.0, C		
	NH amide	8.56, d, (8.9)			
	1	4.49, m	51.8, CH	Trp 2	
	2	3.06, d, (14.8) 3.17, dd, (14.8, 4.1)	27.6, CH ₂	Trp 1, Trp 3	
	3		108.9, C		
	4	7.29, d, (2.0)	125.0, CH		
	NH	11.00, bs		Trp 5	
	5		136.7, C		
	6	7.34, d, (8.1)	118.7, CH		
	7	7.06, m	121.7, CH		
	8	6.97, m	108.9, CH		
9	7.44, m, (8.0)	118.7, CH			
Pipe	10		127.7, C		
	CO		170.9, C		
	1	3.66, m	56.7, CH	Pipe 5	NH Leu
	2	1.45, m, -0.70 m	23.6, CH ₂		NH Leu
	3	0.99, m, 0.78, m	20.7, CH ₂		
	4	1.25 m, 0.50 m	23.9, CH ₂		
Leu	5	4.32 m, 2.10 m	39.4, CH ₂	CO Trp	
	CO		169.6, C		
	NH amide	8.95, d, (8.5)		CO Pipe	
	1	4.53, m	50.3, CH		Pro 4
	2	1.85, m, 1.53, m	38.3, CH ₂		
	3	1.62, m	25.2, CH	CO Leu	
Leu	4	0.81, m	20.6, CH ₃		
	4'	0.90, m	23.9, CH ₃		
	CO		173.5, C		

Marfey's Analysis of Compound **1**

A sample (150 μ g) of compound **1** was dissolved in 0.3 mL of 6N HCl containing 5% of thioglycolic acid and heated at 110 °C for 16 h. The resulting mixture was dried overnight under a N₂ stream. The solid residue was resuspended in 50 μ L of a 1 M NaHCO₃ solution that turned violet. Once the solution stopped fizzing, 150 μ L of L-FDVA (Marfey's reagent, *N*-(2,4-dinitro-5-fluorophenyl)-L-valinamide) was added and the solution turned yellow. The reaction mixture was heated at 40 °C for 40 min till the solution turned red. After that time, the reactions were quenched by dropwise addition of 1N HCl up to the mixture turned yellow again. For the HPLC analysis, 10 μ L of the derivatives solution were added to 40 μ L of acetonitrile and analyzed by LC/MS on an Agilent 1260 Infinity II single quadrupole LC/MS instrument. Separations were carried out on a Waters X-Bridge C18 column (4.6 \times 150 mm, 5 μ m) maintained at 40 °C. A mixture of two solvents, A (10% acetonitrile, 90% water) and B (90% acetonitrile, 10% water), both containing 1.3 mM trifluoroacetic acid and 1.3 mM ammonium formate, was used as the mobile phase under a linear gradient elution mode (25–65% B in 28 min, 65–100% B in 0.1 min, then isocratic 100% B for 4 min) at a flow rate of 1.0 mL/min. The amino acids standards were derivatized

and analyzed following the same methodology described for compound **1**. HPLC traces of these analyses are shown in Figures S12 and S13. Retention times (min) for the observed peaks in the HPLC trace of the L-FDVA-derivatized amino acids standards were as follows: L-Pro: 7.12, β -Ala: 8.02, D-Pro: 9.15, D-Pipe: 11.9, L-Trp: 12.10, L-Ile – L-Leu: 12.10–12.29, L-Pipe: 13.22, D-Trp: 15.2, D-Ile: 18.5, D-Leu: 18.9. Retention times (min) for the observed peaks in the HPLC trace of the L-FDVA-derivatized hydrolysis product of compound **1** were as follows: L-Pro: 6.98, β -Ala: 8.02, L-Trp: 12.10, L-Ile – L-Leu: 12.10–12.29, and L-Pipe: 13.22.

3.5. Biological Assays

3.5.1. *Plasmodium Falciparum* 3D7 Lactase Dehydrogenase in Vitro Assay

The IC₅₀ of pipecolisporin (**1**) was determined in the *P. falciparum* 3D7 lactate dehydrogenase whole parasite assay as previously described [31]. The isolated compound was tested in duplicate on two different occasions to confirm the IC₅₀.

3.5.2. Transgenic *Trypanosoma cruzi* β -D-galactosidase in vitro Assay

The IC₅₀ of **1** was determined in the transgenic *T. cruzi* β -D-galactosidase assay as previously described [32]. The isolated compound was tested in duplicate on two different occasions to confirm the IC₅₀.

3.5.3. MTT/Cell Viability Assay

The cell viability of five different human cancer cell lines was studied based on the MTT (3-(4,5-dimethylthiazol-2-yl)-2,5-diphenyltetrazolium bromide) assay [33]: A549 (lung carcinoma), A2058 (metastatic melanoma), MCF7 (breast adenocarcinoma), MIA PaCa-2 (pancreatic carcinoma), and HepG2 (hepatocyte carcinoma). IC₅₀ of **1** was determined as previously described [34]. The isolated compound was tested as a 12-point dose–response curve ($\frac{1}{2}$ serial dilutions) starting at a concentration of 50 μ M in triplicate.

3.5.4. Antimicrobial Assays

Antimicrobial activity against a panel of human pathogens including MRSA, *A. baumannii*, *E. coli*, *P.aeruginosa*, *C. albicans*, and *A. fumigatus* was performed as previously reported [35]. The isolated compound was tested as a 10-point dose–response curve ($\frac{1}{2}$ serial dilutions) starting at a concentration of 128 μ g/mL in triplicate.

4. Conclusions

Pipecolisporin (**1**), a new pipecolic acid containing hexapeptide, was isolated from cultures of the endophytic fungus *N. orizae*. The compound displayed remarkable antiparasitic activity against *P. falciparum* and *T. cruzi*, with an IC₅₀ value comparable to that of benznidazole, currently used in the treatment of Chagas disease, and no toxicity against a panel of five human carcinoma cell lines. Therefore, the newly isolated peptide can be proposed as a viable starting point for further investigation in vivo towards its potential application in anti-Chagas chemotherapy.

Supplementary Materials: The following are available online at <https://www.mdpi.com/1424-8247/14/3/268/s1>, Figure S1. CF-298113 Solid State Fermentation on BRFT medium after 21 days of incubation at 22 °C; Figure S2. LC-UV (210 nm) chromatogram of pipecolisporin (**1**); Figure S3. ESI-TOF spectrum of pipecolisporin (**1**); Figure S4. UV spectrum of pipecolisporin (**1**); Figure S5. ¹H-NMR (500 MHz, DMSO-*d*₆) spectrum of pipecolisporin (**1**); Figure S6. ¹³C-NMR (125 MHz, DMSO-*d*₆) spectrum of pipecolisporin (**1**); Figure S7. HSQC (DMSO-*d*₆) spectrum of pipecolisporin (**1**); Figure S8. HMBC (DMSO-*d*₆) spectrum of pipecolisporin (**1**); Figure S9. COSY (DMSO-*d*₆) spectrum of pipecolisporin (**1**); Figure S10. TOCSY (DMSO-*d*₆) spectrum of pipecolisporin (**1**); Figure S11. NOESY (DMSO-*d*₆) spectrum of pipecolisporin (**1**); Figure S12. Chromatographic profile of the standard amino acids present in pipecolisporin (**1**) derivatized with L-FDVA; Figure S13. Chromatographic profile of the amino acids from the hydrolysate of pipecolisporin (**1**) derivatized with L-FDVA; Figure S14. Overlay of HSQC NMR spectra of a hydrolysate of pipecolisporin (**1**) (red

and blue NMR signals) and L-Ile standard amino acid (green and yellow NMR signals); Figure S15. Overlay of HSQC NMR spectra of a hydrolysate of pipecolisporin (**1**) (red and blue NMR signals) and L-*allo*-Ile standard amino acid (green and yellow NMR signals); Figure S16. Growth inhibition curve of pipecolisporin (**1**) against *T. cruzi*; Figure S17. Growth inhibition curve of benzimidazole against *T. cruzi*; Figure S18. Growth inhibition curve of pipecolisporin (**1**) against *P. falciparum* 3D7; Figure S19. Growth inhibition curve of chloroquine against *P. falciparum* 3D7; Figure S20. Growth inhibition curves of pipecolisporin (**1**) against human cell lines; Figure S21. *Nigrospora oryzae* CF-298113. Upper surface overview of a 21 days culture after inoculation on (a) Yeast-Malt medium; (b) cornmeal medium; Figure S22. Conidiogenous cells giving rise to conidia. Scale bars: a–c = 10 µm.

Author Contributions: Conceptualization, O.G., and F.R.; Methodology, I.F.-P., V.G.-M., F.A., C.T., C.B.-N. and T.A.M.; Investigation, I.F.-P., V.G.-M., F.A. and T.A.M.; Writing—original draft preparation, I.F.-P. and V.G.-M.; Writing—review and editing, all authors; Supervision, O.G. and F.R.; Funding acquisition, O.G. and F.R. All authors have read and agreed to the published version of the manuscript.

Funding: Financial support was received from the Junta de Andalucía through grant number PY18-RE-0027 and from the Instituto de Salud Carlos III Subdirección General de Redes y Centros de Investigación Cooperativa-Red de Investigación Cooperativa en Enfermedades Tropicales (RICET: RD16/0027/0014, RD16/0027/0015, and RD12/0018/0005), and the Plan Nacional (SAF2016-79957-R). The polarimeter, HPLC, IR, NMR equipment, and plate reader used in this work were purchased via grants for scientific and technological infrastructures from the Ministerio de Ciencia e Innovación [Grants Nos. PCT-010000-2010-4 (NMR), INP-2011-0016-PCT-010000 ACT6 (polarimeter, HPLC, and IR), and PCT-01000-ACT7, 2011-13 (plate reader)].

Institutional Review Board Statement: Not applicable.

Informed Consent Statement: Not applicable.

Data Availability Statement: The data presented in this study are available on request from the corresponding author.

Conflicts of Interest: The authors declare no conflict of interest.

References

1. Nisa, H.; Kamili, A.N.; Nawchoo, I.A.; Shafi, S.; Shameem, N.; Bandh, S.A. Fungal endophytes as prolific source of phytochemicals and other bioactive natural products: A review. *Microb. Pathog.* **2015**, *82*, 50–59. [[CrossRef](#)]
2. Santoyo, G.; Moreno-Hagelsieb, G.; del Carmen Orozco-Mosqueda, M.; Glick, B.R. Plant growth-promoting bacterial endophytes. *Microbiol. Res.* **2016**, *183*, 92–99. [[CrossRef](#)]
3. Vasundhara, M.; Sudhakara Reddy, M.; Kumar, A. Secondary metabolites from endophytic fungi and their biological activities. In *New and Future Developments in Microbial Biotechnology and Bioengineering: Microbial Secondary Metabolites Biochemistry and Applications*; Gupta, V.K., Pandey, A., Eds.; Elsevier: Oxford, UK, 2019; pp. 237–258.
4. Hardoim, P.R.; van Overbeek, L.S.; Berg, G.; Pirttilä, A.M.; Compant, S.; Campisano, A.; Döring, M.; Sessitsch, A. The Hidden World within Plants: Ecological and Evolutionary Considerations for Defining Functioning of Microbial Endophytes. *Microbiol. Mol. Biol. Rev.* **2015**, *79*, 293–320. [[CrossRef](#)] [[PubMed](#)]
5. Ebada, S.S.; Eze, P.; Okoye, F.B.C.; Esimone, C.O.; Proksch, P. The Fungal Endophyte *Nigrospora oryzae* Produces Quercetin Monoglycosides Previously Known Only from Plants. *ChemistrySelect* **2016**, *1*, 2767–2771. [[CrossRef](#)]
6. Ganley, R.J.; Brunsfeld, S.J.; Newcombe, G. A community of unknown, endophytic fungi in western white pine. *Proc. Natl. Acad. Sci. USA* **2004**, *101*, 10107–10112. [[CrossRef](#)] [[PubMed](#)]
7. Vector-Borne Diseases. Available online: <https://www.who.int/news-room/fact-sheets/detail/vector-borne-diseases> (accessed on 17 November 2020).
8. Tajuddeen, N.; Van Heerden, F.R. Antiplasmodial natural products: An update. *Malar. J.* **2019**, *18*, 404. [[CrossRef](#)]
9. Cota, B.B.; Rosa, L.H.; Caligiorme, R.B.; Rabello, A.L.T.; Almeida Alves, T.M.; Rosa, C.A.; Zani, C.L. Altenusin, a biphenyl isolated from the endophytic fungus *Alternaria* sp., inhibits trypanothione reductase from *Trypanosoma cruzi*. *FEMS Microbiol. Lett.* **2008**, *285*, 177–182. [[CrossRef](#)]
10. Tansuwan, S.; Pornpakakul, S.; Roengsumran, S.; Petsom, A.; Muangsin, N.; Sihanonta, P.; Chaichit, N. Antimalarial Benzoquinones from an Endophytic Fungus, *Xylaria* sp. *J. Nat. Prod.* **2007**, *70*, 1620–1623. [[CrossRef](#)]
11. Kontnik, R.; Clardy, J. Codinaeopsin, an Antimalarial Fungal Polyketide. *Org. Lett.* **2008**, *10*, 4149–4151. [[CrossRef](#)]
12. Ibrahim, S.R.M.; Abdallah, H.M.; Elkhayat, E.S.; Al Musayeb, N.M.; Asfour, H.Z.; Zayed, M.F.; Mohamed, G.A. Fusaripeptide A: New antifungal and anti-malarial cyclodepsipeptide from the endophytic fungus *Fusarium* sp. *J. Asian Nat. Prod. Res.* **2018**, *20*, 75–85. [[CrossRef](#)]

13. Annang, F.; Pérez-Moreno, G.; González-Menéndez, V.; Lacret, R.; Pérez-Victoria, I.; Martín, J.; Cantizani, J.; de Pedro, N.; Choquesillo-Lazarte, D.; Ruiz-Pérez, L.M.; et al. Strasseriolides A-D, A Family of Antiplasmodial Macrolides Isolated from the Fungus *Strasseria geniculata* CF-247251. *Org. Lett.* **2020**, *22*, 6709–6713. [[CrossRef](#)]
14. Wang, G.; Liu, Z.; Lin, R.; Li, E.; Mao, Z.; Ling, J.; Yang, Y.; Yin, W.B.; Xie, B. Biosynthesis of Antibiotic Leucinostatins in Bio-control Fungus *Purpureocillium lilacinum* and Their Inhibition on *Phytophthora* Revealed by Genome Mining. *PLoS Pathog.* **2016**, *12*, 1005685. [[CrossRef](#)]
15. Smith, C.M.; Jerkovic, A.; Truong, T.T.; Foote, S.J.; McCarthy, J.S.; McMorran, B.J. Griseofulvin impairs intraerythrocytic growth of *Plasmodium falciparum* through ferrochelataze inhibition but lacks activity in an experimental human infection study. *Sci. Rep.* **2017**, *7*, 41975. [[CrossRef](#)] [[PubMed](#)]
16. Barúa, J.E.; de la Cruz, M.; de Pedro, N.; Cautain, B.; Hermosa, R.; Cardoza, R.E.; Gutiérrez, S.; Monte, E.; Vicente, F.; Collado, I.G. Synthesis of Trichodermin Derivatives and Their Antimicrobial and Cytotoxic Activities. *Molecules* **2019**, *24*, 3811. [[CrossRef](#)] [[PubMed](#)]
17. Guo, B.; Wang, Y.; Sun, X.; Tang, K. Bioactive natural products from endophytes: A review. *Appl. Biochem. Microbiol.* **2008**, *44*, 136–142. [[CrossRef](#)]
18. Linington, R.G.; González, J.; Ureña, L.D.; Romero, L.I.; Ortega-Barría, E.; Gerwick, W.H. Venturamides A and B: Antimalarial constituents of the Panamanian marine cyanobacterium *Oscillatoria* sp. *J. Nat. Prod.* **2007**, *70*, 397–401. [[CrossRef](#)] [[PubMed](#)]
19. Búa, J.; Fichera, L.E.; Fuchs, A.G.; Potenza, M.; Dubin, M.; Wenger, R.O.; Moretti, G.; Scabone, C.M.; Ruiz, A.M. Anti-*Trypanosoma cruzi* effects of cyclosporin A derivatives: Possible role of a P-glycoprotein and parasite cyclophilins. *Parasitology* **2008**, *135*, 217–228. [[CrossRef](#)]
20. Sweeney-Jones, A.M.; Gagaring, K.; Antonova-Koch, J.; Zhou, H.; Mojib, N.; Soapi, K.; Skolnick, J.; McNamara, C.W.; Kubanek, J. Antimalarial Peptide and Polyketide Natural Products from the Fijian Marine Cyanobacterium *Moorea producens*. *Mar. Drugs* **2020**, *18*, 167. [[CrossRef](#)]
21. Lee, Y.; Phat, C.; Hong, S.C. Structural diversity of marine cyclic peptides and their molecular mechanisms for anticancer, antibacterial, antifungal, and other clinical applications. *Peptides* **2017**, *95*, 94–105. [[CrossRef](#)]
22. Stawikowski, M.; Cudic, P. A novel strategy for the solid-phase synthesis of cyclic lipodepsipeptides. *Tetrahedron Lett.* **2006**, *47*, 8587–8590. [[CrossRef](#)]
23. Tanaka, M.; Fukushima, T.; Tsujino, Y.; Fujimori, T. Nigrosporins A and B, New Phytotoxic and Antibacterial Metabolites Produced by a Fungus *Nigrospora oryzae*. *Biosci. Biotechnol. Biochem.* **1997**, *61*, 1848–1852. [[CrossRef](#)] [[PubMed](#)]
24. Ding, L.J.; Yuan, W.; Liao, X.J.; Han, B.N.; Wang, S.P.; Li, Z.Y.; Xu, S.H.; Zhang, W.; Lin, H.W. Oryzamides A-E, Cyclodepsipeptides from the Sponge-Derived Fungus *Nigrospora oryzae* PF18. *J. Nat. Prod.* **2016**, *79*, 2045–2052. [[CrossRef](#)]
25. Ortiz-López, F.J.; Carretero-Molina, D.; Sánchez-Hidalgo, M.; Martín, J.; González, I.; Román-Hurtado, F.; Cruz, M.; García-Fernández, S.; Reyes, F.; Deisinger, J.P.; et al. Cacaoidin, First Member of the New Lanthidin RiPP Family. *Angew. Chem. Int. Ed.* **2020**, *59*, 12654–12658. [[CrossRef](#)]
26. Gonzalez-Menendez, V.; Martin, J.; Siles, J.A.; Gonzalez-Tejero, M.R.; Reyes, F.; Platas, G.; Tormo, J.R.; Genilloud, O. Biodiversity and chemotaxonomy of *Preussia* isolates from the Iberian Peninsula. *Mycol. Prog.* **2017**, *16*, 713–728. [[CrossRef](#)]
27. Blaxter, M.; Mann, J.; Chapman, T.; Thomas, F.; Whitton, C.; Floyd, R.; Abebe, E. Defining operational taxonomic units using DNA barcode data. *Philos. Trans. R. Soc. B Biol. Sci.* **2005**, *360*, 1935–1943. [[CrossRef](#)]
28. Hofstetter, V.; Buyck, B.; Eyssartier, G.; Schnee, S.; Gindro, K. The unbearable lightness of sequenced-based identification. *Fungal Divers.* **2019**, *96*, 243–284. [[CrossRef](#)]
29. Widmer, T.; Kirk, A.; Kirk, G.; Guermache, F. Foliar and Cane Rot of *Arundo donax* Caused by *Nigrospora oryzae* in Europe. *Plant Dis.* **2006**, *90*, 1107. [[CrossRef](#)]
30. Pelaez, F.; Cabello, A.; Platas, G.; Díez, M.T.; Del Val, A.G.; Basilio, A.; Martín, I.; Vicente, F.; Bills, G.F.; Giacobbe, R.A.; et al. The Discovery of Enfumafungin, a Novel Antifungal Compound Produced by an Endophytic *Hormonema* Species Biological Activity and Taxonomy of the Producing Organisms. *Syst. Appl. Microbiol.* **2000**, *23*, 333–343. [[CrossRef](#)]
31. Pérez-Moreno, G.; Cantizani, J.; Sánchez-Carrasco, P.; Ruiz-Pérez, L.M.; Martín, J.; El Aouad, N.; Pérez-Victoria, I.; Tormo, J.R.; González-Menendez, V.; González, I.; et al. Discovery of New Compounds Active against *Plasmodium falciparum* by High Throughput Screening of Microbial Natural Products. *PLoS ONE* **2016**, *11*, e0145812. [[CrossRef](#)]
32. Annang, F.; Pérez-Moreno, G.; García-Hernández, R.; Cordon-Obras, C.; Martín, J.; Tormo, J.R.; Rodríguez, L.; De Pedro, N.; Gómez-Pérez, V.; Valente, M.; et al. High-Throughput Screening Platform for Natural Product-Based Drug Discovery Against 3 Neglected Tropical Diseases: Human African Trypanosomiasis, Leishmaniasis, and Chagas Disease. *J. Biomol. Screen.* **2015**, *20*, 82–91. [[CrossRef](#)]
33. Präbst, K.; Engelhardt, H.; Ringgeler, S.; Hübner, H. Basic colorimetric proliferation assays: MTT, WST, and resazurin. In *Methods in Molecular Biology*; Gilbert, D.F., Friedrich, O., Eds.; Springer Nature: New York, NY, USA, 2017; Volume 1601, pp. 1–17.
34. Koagne, R.R.; Annang, F.; Cautain, B.; Martín, J.; Pérez-Moreno, G.; Thierry, M.; Bitchagno, G.; González-Pacanowska, D.; Vicente, F.; Simo, I.K.; et al. Cytotoxicity and antiplasmodial activity of phenolic derivatives from *Albizia zygia* (DC.) J.F. Macbr. (Mimosae). *BMC Complement. Med. Ther.* **2020**, *20*, 8. [[CrossRef](#)] [[PubMed](#)]
35. Audoin, C.; Bonhomme, D.; Ivanisevic, J.; Cruz, M.D.I.; Cautain, B.; Monteiro, M.C.; Reyes, F.; Rios, L.; Perez, T.; Thomas, O.P. Balibalosides, an Original Family of Glucosylated Sesterterpenes Produced by the Mediterranean Sponge *Oscarella balibaloii*. *Mar. Drugs* **2013**, *11*, 1477–1489. [[CrossRef](#)] [[PubMed](#)]